Identification of key atomic process of Metal-induced lateral crystallization from First-principles Calculations

Yutaro Ogawa
Advanced Memory Development Center, Memory Division, Kioxia Corporation
Yokohama, Japan
yutaro1.ogawa@kioxia.com

Hikari Suzuki
Core Technology Research Center, Frontier Technology R&D Institute, Kioxia Corporation
Yokohama, Japan

Masayasu Miyata
Advanced Memory Development Center, Memory Division, Kioxia Corporation
Yokohama, Japan
masayasu.miyata@kioxia.com

2024 International Conference on Simulation of Semiconductor Processes and Devices (SISPAD) | 979-8-3315-1635-2/24/$31.00 ©2024 IEEE | DOI: 10.1109/SISPAD62626.2024.10733260

***Abstract*—In order to improve the efficiency of metal-induced lateral crystallization (MILC) using Ni, it is important to understand the fundamental mechanisms. In this study, the $NiSi_2$/amorphous Si (a-Si) interface is appropriately modeled and the atom transfer behavior during the MILC process was explored by first-principles calculations. It is found that the overall picture of MILC mechanism can be effectively comprehended through three fundamental processes: (1) the formation of Ni vacancies at the a-Si interface, (2) the diffusion of Ni vacancies within the bulk $NiSi_2$, and (3) the reconstruction of the c-Si interface. The trends under stress, observed in experiments, are explained by applying this mechanism to the MILC process.**

Keywords—Metal-induced lateral crystallization, MILC, crystal silicon, amorphous silicon, nickel disilicide, amorphous interface, density functional theory (DFT), formation energy, Nickel vacancy, diffusion barrier.

I. Introduction

In highly integrated monolithic 3D LSIs, vertical Si channel structures are widely used, from current 3D flash memory cell transistors to future vertical transistors such as VTFETs [1]. In the conventional process, vertical Si channels are embedded in as an a-Si and then transformed to poly-Si at high temperatures to achieve low resistance. One of the most efficient prescription to increase the channel current is the improvement of the crystallinity of Si channel. Metal-induced lateral crystallization (MILC) technology is a feasible candidate for the formation of highly crystalline Si channel [2-4]. On the other hand, since poly-Si is embedded in a solid, the influence of stress from the surroundings is inevitable. To further improve the crystallinity, it is necessary to construct a theoretical model of the MILC phenomenon and predict external effects, such as stress, based on the model. Various experimental [4-7] and theoretical [8-11] investigations of MILC have been widely conducted with TFTs in the area of flat-panel displays, and various models of MILC have been proposed. However, a comprehensive theoretical elucidation of the overall picture of MILC phenomena, which can lead to effective process improvement guidelines, has not been found in the past, due to the inherent complexity of the amorphous interface structures.

In this study, the amorphous interface structure has been appropriately modeled by first-principles calculations, and the overall picture of MILC has been revealed by focusing on the principal phenomena. Fig. 1(a) shows a schematic illustration of MILC growth. The generation of reactive and diffusive species at c-Si/$NiSi_2$ or $NiSi_2$/a-Si interface were assumed. The main atomic species and rate-limiting processes were subsequently identified by examining the reactivity and diffusivity of $NiSi_2$ at each interface. Based on these results, the effects of stresses on MILC were predicted for an instance of external effects.

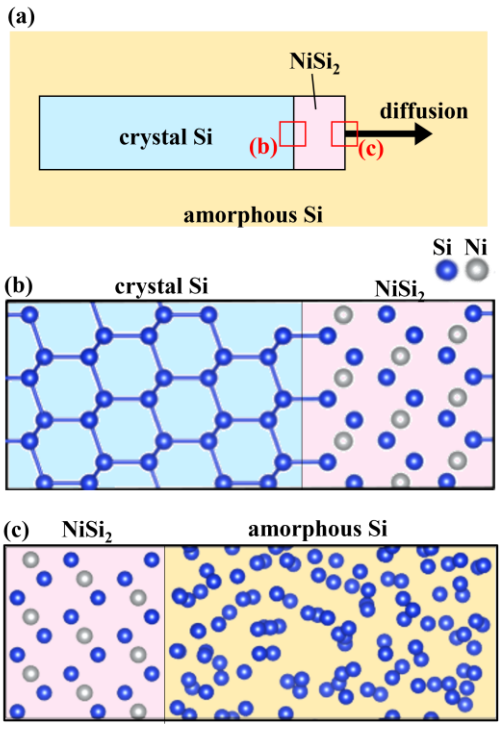

Fig. 1. (a) Schematic illustration of MILC growth. Interface models of (b) crystal Si/ $NiSi_2$ and (c) $NiSi_2$/amorphous Si, corresponding to each region (b), (c) highlighted in the red in (a), respectively.

II. Method and Models

Structural relaxation and finite temperature molecular dynamics (MD) calculations were performed with DFT using

the first-principles calculations software PHASE/0 [12]. We adopted the Perdew-Burke-Ernzerhof parameterization of generalized gradient approximation [13] for the electronic structure calculation. The plane wave basis sets were employed together with the projector augmented wave potential [14]. The cutoff energy of the wavefunction was set to be 30 Hartree. To ensure convergence, energy for the self-consisted field calculations and forces were required to reach a threshold of 1×10^{-5} eV and 5×10^{-3} eV/Å, respectively. For Brillouin zone integration, Γ point was only used for the MD calculation and 2×2×1 Monkhorst-Pack grid [15] was employed in the structural optimizations. To investigate atomic reaction process, the nudged elastic band method was used. The effect of stress was evaluated by calculating the change in energies. Uniaxial strains from –0.7% to +0.7% in the direction of MILC growth was applied to the interface models, while allowing relaxation in the other axial directions.

Fig. 1(b) shows a c-Si/$NiSi_2$ interface model consisting of 171 atoms with $NiSi_2$ (111) surface and Si (111) surface of 3×3 size joined to each other [11]. $NiSi_2$/a-Si interface models were obtained by melt-quenching only the c-Si region of the interface model, starting from 2000 K and quenching at the rate of by -1.0×10^{14} K/s. This MD calculation was carried out using Nosé-Hoover thermostat method [16, 17]. The interface model requires a large number of atoms to avoid structural changes, such as irregular coordination in amorphous due to interface stress. However, performing first-principle simulation with such a large number of atoms is not feasible with respect to computational resources. Therefore, the minimum necessary size must be found. To obtain an appropriate amorphous interface model, eight different models were created to account for the size dependence. The initial c-Si/$NiSi_2$ was set to 2×2 or 3×3, and the thicknesses of the c-Si region were changed from 6 to 12 atomic layers.

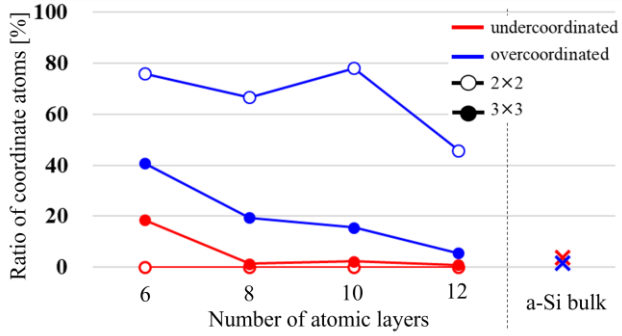

Fig. 2. Coordination number distribution of Si atoms in the $NiSi_2$/a-Si interface models and a-Si bulk model. The interface size was 2×2 (open) or 3×3 (closed), and the thickness of the Si region was varied from 6 to 12 atomic layers in the model. The values of a-Si bulk (cross) was calculated by a 64-atoms a-Si model.

Fig. 2 shows the relationship between the size of $NiSi_2$/a-Si interface model and the ratio of irregularly coordination of Si atoms in each a-Si region. It was observed that the ratio of irregular coordination Si atoms in the 2×2 interface model did not reach the ratio in a-Si bulk model. On the other hand, as the size of the model increased, the ratio in the 3×3 interface model approached that of the bulk a-Si model. Thus 3×3 interface and 12 layers was sufficient condition and adopted in this study. The size of the model is shown in Fig. 1(c).

III. Results

During MILC proceeds, the region of c-Si increases and that of a-Si decreases, as the mass flow rate at the c-Si interface should be balanced with that at the a-Si interface. In general, disorder of interfaces makes diffusive species and diffusion pathways complex. However, it is effective approach to understand key atomic processes from ideal systems. Therefore, we focused on the behavior of single atoms on ideal interfaces like Fig. 1(b), (c). The elemental processes involved in MILC should consist of atomic diffusions of Ni, Si atoms or vacancies.

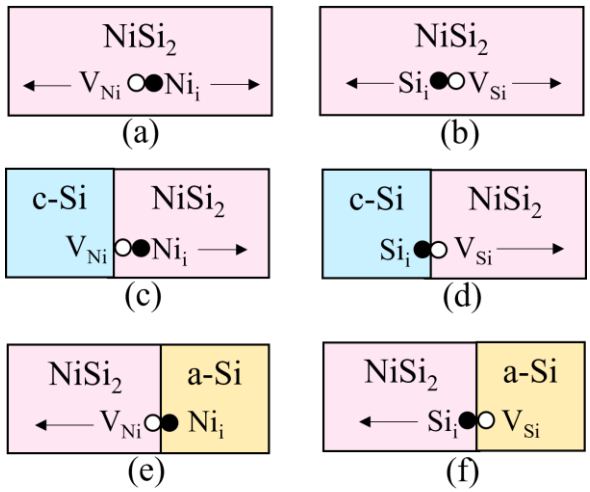

Fig. 3. Possible formation process in MILC of diffusive species. Ni or Si atoms (filled circle) and vacancies (open circle) were formed. (a) Interstitial and vacancy pair of Ni and (b) the pair of Si in $NiSi_2$ bulk. (c) Interstitial Ni and (d) Si vacancy formed at c-Si/$NiSi_2$. (e) Ni vacancy and (f) interstitial Si formed at $NiSi_2$/a-Si. The diffusions indicated by the arrow were calculated for their barrier energies.

Fig. 3 shows the possible formation processes of these diffusive species, similar to the Frenkel defect. The formation of these species at $NiSi_2$ bulk (Fig. 3(a), (b)), c-Si/$NiSi_2$ interface (Fig. 3(c), (d)) and $NiSi_2$/a-Si interface (Fig. 3(e), (f)) were examined. To investigate the energetics of these processes, the values of formation energy (E_f) of the interstitial atoms and the vacancies in $NiSi_2$ region were calculated. E_f for the Frenkel pair of X(=Ni, Si) in $NiSi_2$ bulk region were defined as,

$$E_f = E_{\text{bulk, V}_X} + E_{\text{bulk, X}_i} - 2E_{\text{bulk, pristine}} \quad (1)$$

where $E_{\text{bulk, pristine}}$, $E_{\text{bulk, Vx}}$, $E_{\text{bulk, Xi}}$ are the calculated ground-state energy of the $NiSi_2$ bulk pristine model, the model with a X vacancy and a interstitial X, respectively. The values of E_f in the both interfaces were also defined as,

$$E_f = E_{\text{interface, X}_I+\text{V}_X} - E_{\text{interface, pristine}} \quad (2)$$

where $E_{\text{interface, pristine}}$, $E_{\text{interface, Vx+Xi}}$ are the calculated energy of the pristine interface model (Fig. 1(b) or (c)), the model with a

pair of a X vacancy and a interstitial X, respectively. For $NiSi_2$/a-Si interface, E_f were averaged over nine different configurations. Table.1 shows the lowest value of E_f for each species, with Ni vacancy (V_{Ni}) having the lowest E_f. This suggests that V_{Ni} is the most easily formed at $NiSi_2$/a-Si interface and dominant diffusing species in MILC.

TABLE I. FORMATION ENERGIES OF SPECIES BY CALCULATION

	Formed at	E_f [eV]
Frenkel pair of Ni	$NiSi_2$ bulk	2.8
Frenkel pair of Si		3.7
Interstitial Ni	c-Si/$NiSi_2$	2.8
Si vacancy		3.9
Ni vacancy	$NiSi_2$/a-Si	**1.5**
Interstitial Si		5.1

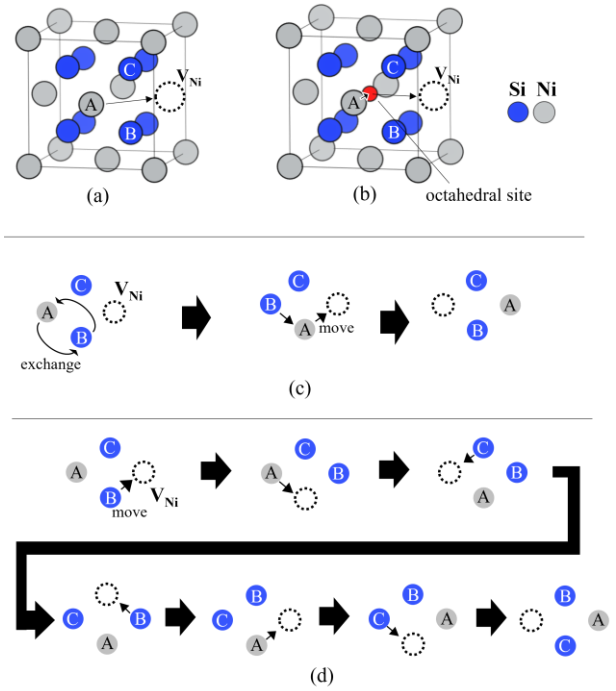

Fig. 4. Four diffusion paths showing a single Ni atom (gray, labeled A) moving towards V_{Ni} sites (dotted open) in $NiSi_2$ bulk region. (a) Ni atom moves straight between two Si atoms (labeled B and C). (b) Ni atom moves through the octahedral site (colored red). (c) A schematic diagrams illustrating two-step and (d) six-step diffusion path of Ni atom collaborating with Si atoms.

Next, the diffusion behavior of V_{Ni} was examined to obtain an overall picture of MILC. Possible four different types of diffusion paths were investigated to find the path as smaller energy barrier as possible. Fig. 4(a) shows the pathway where Ni atom moves straight between two Si atoms. In Fig. 4(b), Ni atom moves through an adjacent octahedral site. In Fig. 4(c), Ni atom exchanges positions with its neighboring Si atom, and then moves towards V_{Ni} site. In Fig. 4(d), Ni atom moves in six steps of atomic sequential exchanges with a vacancy and two Si atoms [18]. Each diffusion path shown in Fig. 4 has diffusion barrier (E_a) of (a) 4.1 eV, (b) 2.6 eV, (c) 3.8 eV, (d) 1.9 eV, respectively. Based on these calculations, the dominant diffusion path for Ni in $NiSi_2$ bulk region is the six-step pathway shown in Fig. 4(d).

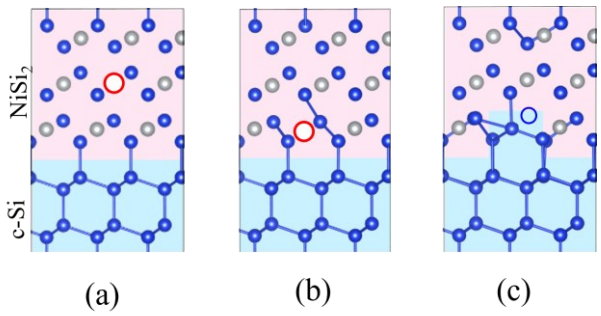

Fig. 5. Ni vacancy aggregates at the c-Si/$NiSi_2$ interface and the interface is reconstructed and transformed to Si. (a) V_{Ni} is in $NiSi_2$ bulk region. (b) V_{Ni} diffuses to the interface. (c) Finally Si atom moves to the V_{Ni} site and new Si region increases.

Atomic mechanism of c-Si growth in MILC is proposed in [10]. This process requires the reconstruction of the interface. Fig. 5 shows the lattice matched interface of $NiSi_2$ and c-Si. Fig. 5(a) shows the initial interface configuration including a single V_{Ni}. The V_{Ni} reaches to the interface (Fig. 5(b)) and exchange the position with a nearest neighbor Si atom (Fig. 5(c)), which results in the growth of the c-Si region. The value of E_a for this reconstruction process was calculated as the Si atom diffusion from Fig. 5(b) to Fig. 5(c).

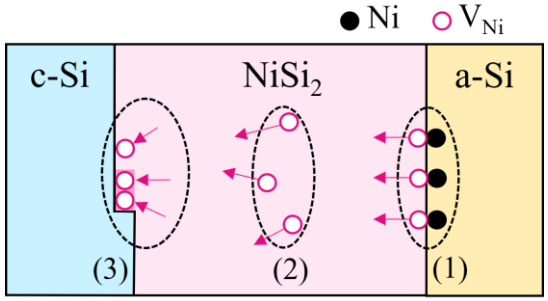

Fig. 6. Reaction-diffusion processes of Ni vacancy in MILC. (1) Formation as a Frenkel pair at the a-Si interface, (2) diffusion in the $NiSi_2$ bulk, and (3) aggregation at the c-Si interface, interface reconstruction, and epitaxial growth of new Si (111).

TABLE II. DIFFUSION BARRIERS OF NI VACANCY FOR EACH ELEMENTARY PROCESS IN MILC.

	E_a [eV]	
	This study	*Exp.* [8]
Formation at $NiSi_2$/a-Si	1.6	1.9-2.1
Diffusion in $NiSi_2$ bulk	**1.9**	
Reconstruction of c-Si/$NiSi_2$	1.1	

Fig. 6 shows the overview of the entire process of MILC derived from considering V_{Ni} as the key species. The process can be summarized as follows: (1) Formation of V_{Ni} as a Frenkel pair at the a-Si interface, (2) diffusion of V_{Ni} in the bulk $NiSi_2$, and (3) aggregation of V_{Ni} at the c-Si interface, leading to the epitaxial growth of new Si (111) surface by interface reconstruction process. Table 2 shows the E_a associated with each process (1)-(3). It is revealed that the rate-limiting step is the diffusion of V_{Ni} in $NiSi_2$ bulk region. The calculated E_a is

consistent with the experimental value [8], evaluated from crystallization growth rate. This good agreement supports the validity of the model shown in Fig. 6. Identification of key atomic process including diffusive species and diffusion pathway by calculation allows us to clarify atomic processes in MILC that have been black boxes in experiments.

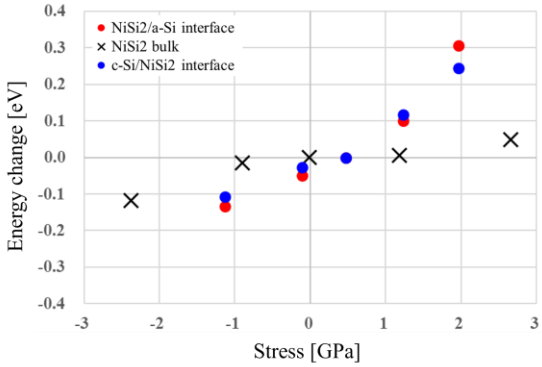

Fig. 7. Change in the sum of Ni vacancy formation energy and diffusion barrier in the bulk and at the interfaces. Here, the negative direction of stress indicates tensile and the positive direction indicates compressive stress.

Based on the above mechanism, we investigated how accurately the key atomic process can predicts the effect of stress on MILC. Uniaxial stress in the direction of MILC growth was applied to the interface models in Fig. 1(b), (c) and $NiSi_2$ bulk model. Diffusion coefficient D in the case of atomic diffusion collaborating with a vacancy is formulated by Fick's laws;

$$D = D_0 \, e^{-\frac{E_f}{k_B T}} e^{-\frac{E_a}{k_B T}} \tag{3}$$

where the formation energy E_f for V_{Ni}, the energy barrier of diffusive atom E_a and a constant D_0. Eq. 3 shows the diffusion of V_{Ni} depends on the sum of E_f and E_a. Fig. 7 shows that stress dependency of the sum of the energies at the both interfaces and $NiSi_2$ bulk model were calculated. Uniaxial tensile stress reduces the sum of energies in the $NiSi_2$ bulk, especially at the both interface. These results suggest that MILC can be accelerated by applying tensile stress in the direction of MILC growth. Furthermore, these results also correspond to experimentally observed trends due to the effect of stress on MILC growth rate [19, 20]. The agreement between the experimental and theoretical tendency under stress supports the model shown in Fig. 6.

IV. Conclusions

In this study, the progression mechanism of the MILC process was clarified by first-principles calculations. It was found that the MILC mechanism can be understood as a sequence of three elementary processes: (1) Formation of V_{Ni} as a Frenkel pair at the a-Si interface, (2) diffusion of V_{Ni} in the bulk $NiSi_2$, and (3) aggregation of V_{Ni} at the c-Si interface, leading to the epitaxial growth of Si on the (111) surface by interface reconstruction. Furthermore, the effect of uniaxial stress on MILC was also examined, and can effectively promote MILC growth by applying stress appropriately.

Acknowledgment

We would like to thank Shinji Mori for helpful comments and discussions.

References

[1] H. Jagannathan et al., IEDM pp.557-560 (2021).

[2] H. Miyagawa et. al., "Metal-Assisted Solid-Phase Crystallization Process for Vertical Monocrystalline Si Channel in 3D Flash Memory", 2019 IEEE International Electron Devices Meeting, pp.650-653.

[3] N. Ishihara et. al., "Highly Scalable Metal Induced Lateral Crystallization (MILC) Techniques for Vertical Si Channel in Ultra-High (> 300 Layers) 3D Flash Memory", 2023 IEEE Symposium on VLSI Technology and Circuits, T7-1.

[4] H. Matsuo et al., "The Effect of Crystallinity of Channel Silicon Formed by Two Different Metal Induced Lateral Crystallization (MILC) on Cell Current Distribution in 3D Flash Memory", 2023 International Conference on Solid State Devices and Materials, E-4-03.

[5] C. Hayzelden et al., "Silicide formation and silicide-mediated crystallization of nickel-implanted amorphous silicon thin films", J. Appl. Phys., 73, 8279 (1993).

[6] B. Pécz et al., "Structural Characteristics of the Si Whiskers Grown by Ni-Metal-Induced-Lateral-Crystallization", Nanomaterials, 11, 1878 (2021).

[7] N. Vouroutzis et al., "Structural characterization of poly-Si Films crystallized by Ni Metal Induced Lateral Crystallization", Sci. Rep. 9, 2844 (2019).

[8] G. Z. Radnóczi et al., "Structural characterization of nanostructures grown by Ni metal induced lateral crystallization of amorphous-Si", J. Appl. Phys., 119, 065303 (2016).

[9] J.-S. Ahn et al., "The effect of dopants on the microstructure of polycrystalline silicon thin film grown by MILC method", Journal of Crystal Growth, 290 (2006) 379-383.

[10] J.-S. Ahn et al., "Effect of MSi2/Si(111) (M = Co, Ni) interface structure on metal induced lateral crystallization", Thin Solid Films, 542, 426-429 (2013).

[11] F. Fuchs et al., "Formation and crystallographic orientation of NiSi2–Si interfaces", J. Appl. Phys., 128, 085301 (2020).

[12] T. Yamasaki, et al., "Multi-axis Decomposition of Density Functional Program for Strong Scaling up to 82,944 Nodes on the K Computer: Compactly Folded 3D-FFT Communicators in the 6D Torus Network" Comput. Phys. Comm. 244, 264-276 (2019).

[13] J. P. Perdewet al., "Generalized gradient approximation made simple", Phys. Rev. Lett., vol. 78, pp. 1396, 1997.

[14] P. E. Blöchl, "Projector augmented-wave method", Phys. Rev. B 50, 17953 (1994).

[15] H. J. Monkhost and J. D. Pack, "Special points for Brillouin-zone integrations", Phys. Rev. B 13, 5188 (1976).

[16] S. Nosé, "A unified formulation of the constant temperature molecular-dynamics methods". J. Chem. Phys. 81, 511-519 (1984).

[17] W. G. Hoover, "Canonical dynamics: Equilibrium phase-space distributions". Phys. Rev. A 31, 1965 (1985).

[18] H. B. Huntington et al., "Self-diffusion in 50-50 Gold-Cadmium Autodiffusion dans un alliage 50-50 or-cadmium Selbstdiffusion in 50-50 Gold-Kadmium", Acta Met., 9, 8 (1961).

[19] C.-Y. Hou et al., "Effects of Tensile Stress on Growth of Ni–Metal-Induced Lateral Crystallization of Amorphous Silicon", Jpn. J. Appl. Phys., 44, 7327 (2005).

[20] S. Y. Huang et al., "Effect of compressive stress on nickel-induced lateral crystallization of amorphous silicon thin films", Thin Solid Films, 520 (2021) 2984.